

## Monitoring Skin Temperature during Hand-Object Interactions

Hsin-Ni Ho<sup>1,2</sup> and Lynette A. Jones<sup>1</sup>

<sup>1</sup>Department of Mechanical Engineering, Massachusetts Institute of Technology, Cambridge, MA, USA

<sup>2</sup>NTT Communication Science Laboratories, NTT Corporation, Atsugi, Kanagawa, Japan

### ABSTRACT

An IR thermal measurement system was created to monitor skin temperature during hand-object interactions. The layout and optical arrangement of the system allowed for the measurement of skin temperature across the fingerpad during contact, together with contact force and contact area. An IR model was developed to compensate for the effects of the optical components that were placed between the fingerpad and IR camera. Based on this model, the measured thermal energy could be converted into a temperature distribution on the fingerpad during contact. The performance of this system was evaluated with calibration tests and the results indicated that this system was capable of providing accurate temperature measurements without the limitations imposed by conventional thermal sensors. Measurements obtained with this system can be used to evaluate the validity of models used to predict the changes in skin temperature during hand-object interactions.

### INTRODUCTION

Modeling the thermal responses that occur when the hand makes contact with an object is essential for developing thermal feedback systems for haptic displays. When evaluating a thermal model from a physiological perspective, the temperature responses of the skin during contact are typically measured with small thermal sensors, such as thermistors or thermocouples affixed to the skin. However, it is difficult to obtain consistent temperature measurements with sensors. When the sensor is placed directly on the contact area [1, 2], it molds to the fingerpad and affects the surface area between the fingerpad and material. When it is attached to the perimeter of the contact area [3, 4], the localized nature of the change in skin temperature means that the sensor is not able to detect the full extent of the temperature change during contact. As a result, there are considerable differences in the magnitude of the changes in skin temperature recorded as a function of the location of the thermal sensor, with larger decreases reported when the sensor is directly on the contact area as shown in Figure 1. In addition, the measured time courses and amplitude of the skin temperature changes during contact are significantly different from theoretical predictions [5].

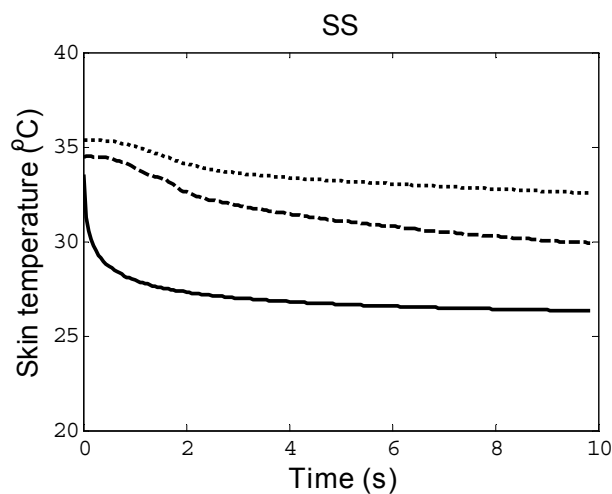
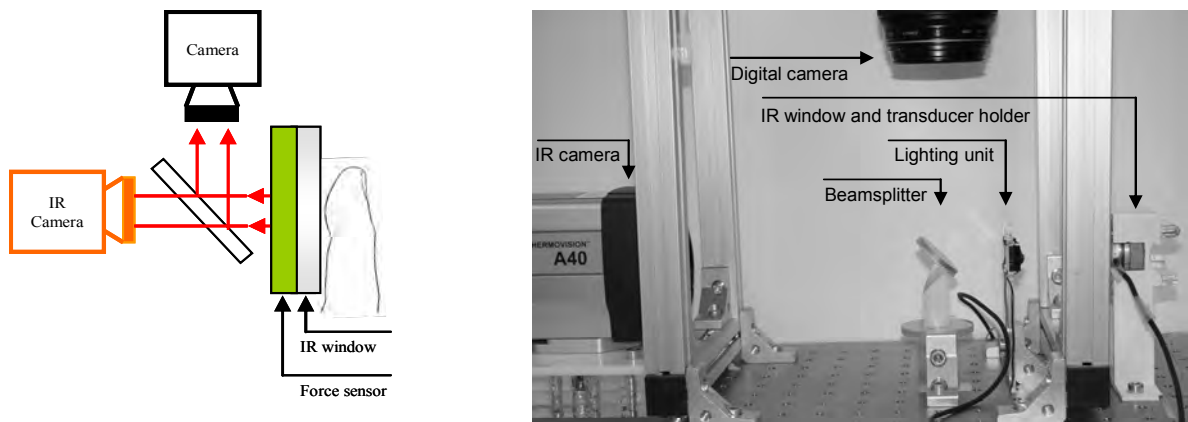


Figure 1. Changes in skin temperature during contact with stainless steel with the sensor attached to the center (dashed line) or perimeter (dotted line) of the contact area. Model predictions from Ho and Jones [5] are also shown (solid line).

It is unclear whether the discrepancies between the predicted and measured changes in skin temperature reflect the limitations imposed by thermal sensors or inadequacies in the thermal model. A clearer understanding of the thermal response of the skin to contact would be possible if a non-contact thermal measurement system was used. As a result, an infrared thermal measurement system has been developed to provide an image of the temperature distribution across the fingerpad during contact. This system has been designed so that it can measure contact area, contact force and the change in skin temperature simultaneously during contact. These measurements permit the validation of thermal models, which can be incorporated into haptic displays to provide thermal feedback.

## SYSTEM LAYOUT

When an infrared camera is used to measure skin temperature during contact, the optical components placed between the infrared camera and the fingerpad must be infrared transmissive to prevent the obstruction of the thermal radiation emitted from the fingerpad. The layout of the system designed to fulfill these requirements is shown in Figure 2. An infrared camera (A40M, FLIR Systems) was used to measure the thermal radiation emitted from the fingerpad. In order to measure the contact area and temperature distribution on the fingerpad simultaneously, a ZnS infrared window that can transmit wavelengths in both the visible and infrared spectrum was selected as the contact material. It was 43 mm in diameter and 10 mm thick. A beamsplitter, made of Ge with an anti-reflection coating, was used to separate the infrared radiation and visible light from the contact area. It measured 32 mm in diameter, was 3 mm thick and was held at a 45° inclination. The contact area was captured by a digital camera (EOS D60, Canon). A 6-axis force transducer (Nano 43, ATI Industrial Automation) with a 20-mm diameter hole in the center was attached to the contact material and measured the contact force without obscuring the infrared and visible radiation from the fingerpad. During measurement, the distance between the fingerpad and the infrared camera was 300 mm, which was the minimum distance required for focusing. The overall setup of the infrared thermal measurement system is shown in Figure 2.



*Figure 2. Layout of the infrared thermal measurement system.*

## PARAMETERS IN INFRARED MEASUREMENT

In this thermal measurement system, the radiation measured by the infrared camera not only originates from the fingerpad, but also from the surroundings and the optics placed in between the camera and finger. To measure the fingerpad temperature accurately, it was necessary to establish an IR model which compensated for the effects of the different radiation sources. In order to achieve this goal, the following optical parameters needed to be considered.

### Target parameters

The fingerpad was the target of this thermal measurement system. In this study, the fingerpad was a gray body with a constant emissivity of 0.95 [6] within the spectral range of the infrared camera, that is 7.5-13  $\mu\text{m}$ . A calibration test was conducted with the system to validate this assumption which will be discussed later.

### Ambient parameters

Together, the target distance, relative humidity, and ambient temperature determine the transmission of the air between the target and the infrared camera. The total transmissivity of the atmosphere over a distance is

$D = T_m \times T_s$ , where  $T_m$  is the molecular absorption by constituent gases and  $T_s$  is scattering by particles in the atmosphere. In the present configuration, the target distance was 300 mm and therefore the transmissivity of the atmosphere equals 1 [7]. The ambient temperature determines the amount of thermal radiation from the surrounding sources.

## External optics parameters

The infrared camera selected for this system measures over the waveband of 7.5 to 13  $\mu\text{m}$ . In order to characterize the optical properties of the external optics in this spectral range, that is the contact materials and beamsplitter, the spectral transmissivity and reflectivity of the optics were measured with a spectrometer (Nicolet Magna 860 Fourier Transform Infrared Spectrometer). The angles of incidence for the measurement were chosen to be the same as the system configuration, that is normal and 45° for the contact material and beamsplitter, respectively.

The optics used in the system were real body radiators and exhibited a bandpass transmissivity that depended on the waveband response of the infrared camera, the spectral response of the optics, and the temperatures of the optics and the target. Based on the model proposed by Madding [8, 9] with the assumptions that the surfaces of the target and optics were diffuse and that the optics' temperature equaled the ambient temperature, the bandpass transmissivity,  $\tau$ , can be estimated from:

$$\tau = \frac{\int_{7.5}^{13} \tau(\lambda) \cdot R_{\text{det}}(\lambda) \cdot [E(\lambda, T_{\text{tar}}) - E(\lambda, T_{\text{amb}})] d\lambda}{\int_{7.5}^{13} R_{\text{det}}(\lambda) \cdot [E(\lambda, T_{\text{tar}}) - E(\lambda, T_{\text{amb}})] d\lambda} \quad (1)$$

where  $\tau$  is transmissivity,  $R_{\text{det}}$  is the detector response of the infrared camera,  $E$  is the spectral emissive power of a blackbody,  $\lambda$  is wavelength, and  $T$  is temperature in Kelvin. Subscripts tar and amb represent target and ambient, respectively.

The bandpass reflectivity  $\rho$ , is defined as the fraction of the spectral irradiation that is reflected by the surface [6]. With respect to the reflectivity of optics at the infrared camera side, the ambient radiation was assumed to be the only source of irradiation. With the assumption that the surface of the optics is diffuse, the bandpass reflectivity can be calculated from:

$$\rho = \frac{\int_{7.5}^{13} \rho(\lambda) E(\lambda, T_{\text{amb}}) d\lambda}{\int_{7.5}^{13} E(\lambda, T_{\text{amb}}) d\lambda} \quad (2)$$

By working with the bandpass properties of the optics, the optics can be treated as gray bodies within the infrared camera's spectral range. The bandpass emissivity,  $\varepsilon$ , can therefore be estimated from the relation  $\varepsilon + \tau + \rho = 1$ . For a typical hand-object interaction with the initial temperatures of the skin and object of 34 and 24 °C, respectively, the skin surface temperature after 10 seconds of contact should be around 27 °C based on the thermal model proposed by Ho and Jones [5]. The bandpass optical properties of this system were therefore evaluated based on the ambient and target temperature of 24 and 27 °C, respectively.

## IR MODEL FOR TARGET TEMPERATURE DERIVATION

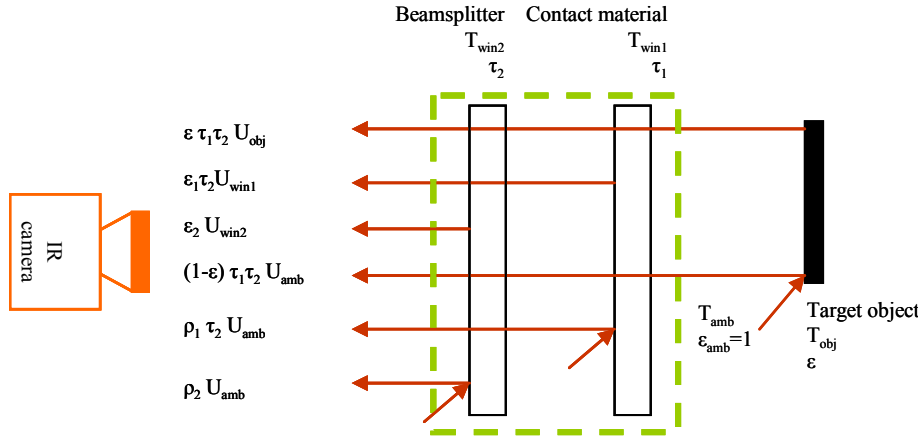


Figure 3. Schematic representation of the IR model.

In order to derive the temperature of the fingerpad during contact based on the thermal energy measured by the infrared camera, an IR model was developed to compensate for the effects of the contact material and beamsplitter placed between the fingerpad and IR camera. The schematic representation of the IR model is shown in Figure 3. This model takes into account various sources of thermal radiation that can be detected by the IR camera. They include the radiation emitted by the contact material, beamsplitter, and target, as well as the ambient radiation reflected by the contact material, beamsplitter and the target. Based on this model, the radiation emitted by the target can be derived as:

$$U_{tot} = \epsilon_{obj} \tau_1 \tau_2 U_{obj} + (1 - \epsilon_{obj}) \tau_1 \tau_2 U_{amb} + \epsilon_2 U_{opt2} + \epsilon_1 \tau_2 U_{opt1} + \rho_1 \tau_2 U_{amb} + \rho_2 U_{amb}$$

$$\Rightarrow U_{obj} = \frac{U_{tot} - (1 - \epsilon_{obj}) \tau_1 \tau_2 U_{amb} - \epsilon_2 U_{opt2} - \epsilon_1 \tau_2 U_{opt1} - \rho_1 \tau_2 U_{amb} - \rho_2 U_{amb}}{\epsilon_{obj} \tau_1 \tau_2} \quad (3)$$

Where  $U$  is the energy signal received by the infrared camera,  $\epsilon$  is emissivity,  $\tau$  is transmissivity, and  $\rho$  is reflectivity. Subscripts tot, obj, amb, and opt stand for total, object, ambient, and optics, respectively, and 1 and 2 represent the contact material and beamsplitter, respectively. The infrared camera measures the total energy signal,  $U_{tot}$ . The infrared camera calibration curve provided by the camera manufacturer enables the conversion between temperature and energy signal. The energy signals of the ambient and optics,  $U_{amb}$  and  $U_{opt}$ , could therefore be estimated from their corresponding temperatures. Based on the model and the calibration curve, the temperature of the target was calculated from  $U_{obj}$ .

### CALIBRATION TESTS

The performance of this system was evaluated with two calibration tests that compared the temperature readings from a thermal sensor with those measured by the thermal measurement system.

**Apparatus.** Although the overall average emissivity of the skin is a generally accepted value, it may vary across different subjects. Using only a single subject's fingerpad as the target in the calibration test might introduce variability into the system and make it difficult to evaluate its performance. In order to have a better control of the target emissivity, standard black insulation tape (Scotch Super 33+, 3M) with an emissivity similar to the skin (0.95) was used to simulate the fingerpad surface in the first set of calibration tests. The tape was attached to a Peltier device (DT6-6, Marlow) and its surface temperature was controlled using a digital PI control system. In the second part of the test, the subject's fingerpad was used as the target. Three thermistors (Model 56A1002-C8, Alpha Technics) were used to monitor the temperatures necessary to derive

the target temperature. These were the ambient temperature and the temperatures of the contact material and beamsplitter.

**Procedure.** An emissivity check was conducted to verify that the overall average emissivity of the target was adequately characterizing its spectral emissivity within the system's range (7.5 – 13  $\mu\text{m}$ ), and to make sure that the system setup did not obscure any thermal radiation that passed through it. This check was done by measuring the target temperature without the contact material and beamsplitter in place. Five target temperatures ranging between 28 and 36  $^{\circ}\text{C}$  were selected for this emissivity check. Each target temperature was repeated three times for a total of 15 trials. The target was placed 10 mm in front of the contact material. For each trial, the temperature of the target was measured with a thermistor and the thermal measurement system simultaneously. The ambient temperature was measured with a thermistor in free air and  $U_{\text{amb}}$  could then be calculated based on the calibration curve. After the emissivity check was done, the contact material and beamsplitter were placed in their corresponding fixtures for the evaluation of the system's performance. Six target temperatures ranging from 27 to 32  $^{\circ}\text{C}$  were chosen, with 5 repetitions of each temperature, which gave a total of 30 trials. On each trial, the temperature of the target was simultaneously measured with a thermistor and the thermal measurement system. The ambient temperature and temperatures of the optics were measured with three thermistors.  $U_{\text{amb}}$ ,  $U_{\text{opt1}}$  and  $U_{\text{opt2}}$  could then be calculated based on those temperatures and the calibration curve.

In the second part of the experiment, the fingerpad was the target. A thermistor was glued to the center of the right index fingerpad using biocompatible cyanoacrylate (Liquid Bandage™, Johnson & Johnson). The emissivity check was done with a procedure similar to the one described above, except that the fingerpad temperature was not controlled. There were 15 trials for each subject. After the emissivity check was done, the system's performance in measuring temperature was evaluated using the fingerpad as a target. Two subjects participated in this test which used a procedure similar to that described above, except that the fingerpad temperature was not controlled. A thermistor was glued to the center of the right index fingerpad. There were 90 trials and on each trial the subject's fingerpad was placed in front of the contact material without touching it. The temperature of the fingerpad was measured with a thermistor and the thermal measurement system simultaneously. The ambient temperature and temperatures of the optics were measured with three other thermistors to estimate  $U_{\text{amb}}$ ,  $U_{\text{opt1}}$  and  $U_{\text{opt2}}$ .

## RESULTS

The results of the emissivity check for the standard black insulation tape and fingerpad are shown in Figure 4(A). The target temperature was the temperature controlled by the Peltier device. The calculated temperature was established from the tape emissivity and the following formula, which is based on the thermal radiation measured by the infrared camera:

$$U_{\text{tot}} = \epsilon_{\text{obj}} U_{\text{obj}} + (1 - \epsilon_{\text{obj}}) U_{\text{amb}}$$

$$\Rightarrow U_{\text{obj}} = \frac{U_{\text{tot}} - (1 - \epsilon_{\text{obj}}) U_{\text{amb}}}{\epsilon_{\text{obj}}} \quad (4)$$

This formula assumes that the thermal radiation received by the infrared camera consisted of the energy emitted by the target and the ambient thermal energy reflected by the target. Based on the calibration curve, the target temperature can be calculated from  $U_{\text{tot}}$ . As shown in Figure 4(A), the intercept of the regression line was set to zero and the slope of the regression line was very close to 1 with a high  $r$  value. This indicated that the system was able to measure the target temperature, accurately given the emissivity of the tape and the formula described in Equation 4. This result further confirmed that the fixtures placed between the target and the infrared camera did not block or affect the thermal energy from the target and surroundings. Although the temperature and the emissivity of the fingerpad was not as uniform as the insulation tape, the result of the emissivity check of the fingerpad shown in Figure 4(B) indicated that the overall average emissivity of the skin was able to provide accurate temperature readings.

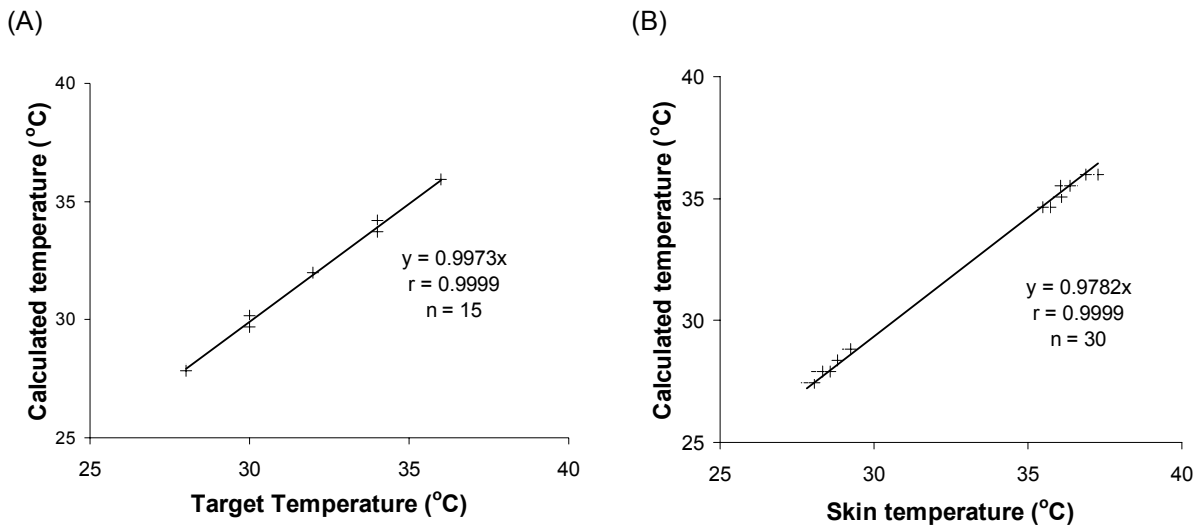


Figure 4. Result of emissivity check for black insulation tape (A) and fingerpad (B).

After verifying that the overall average emissivity of the insulation tape and skin was appropriate for characterizing their spectral emissivity within the system's range (7.5 – 13  $\mu\text{m}$ ), the performance of the system was then evaluated with these targets. The results of the evaluation with the insulation tape are shown in Figure 5(A). The target temperature was the temperature measured by the thermistor and the calculated temperature was derived based on the measured thermal energy and the proposed IR model. With the intercept of the regression line set to zero, the slope calculated from these data was close to 1 (1.03), with a correlation of 0.97 between the measured and calculated target temperature. The system's performance with the fingerpad as the target is shown in Figure 5(B). The results were similar to those with the insulation tape and indicated that the system was able to provide accurate temperature readings. The slope of the regression line was again close to 1 (1.04), with a correlation between the measured and calculated skin temperature of 0.92.

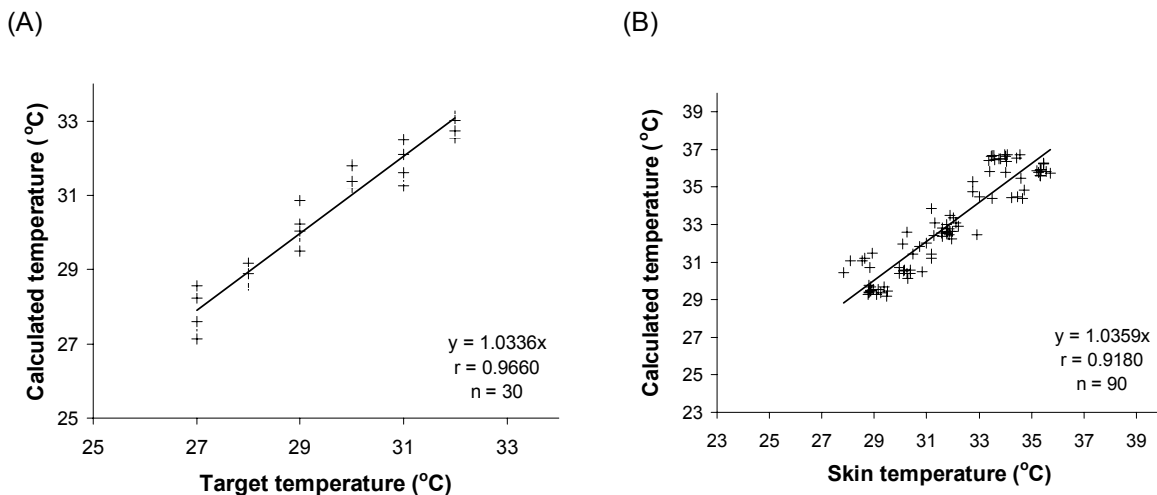
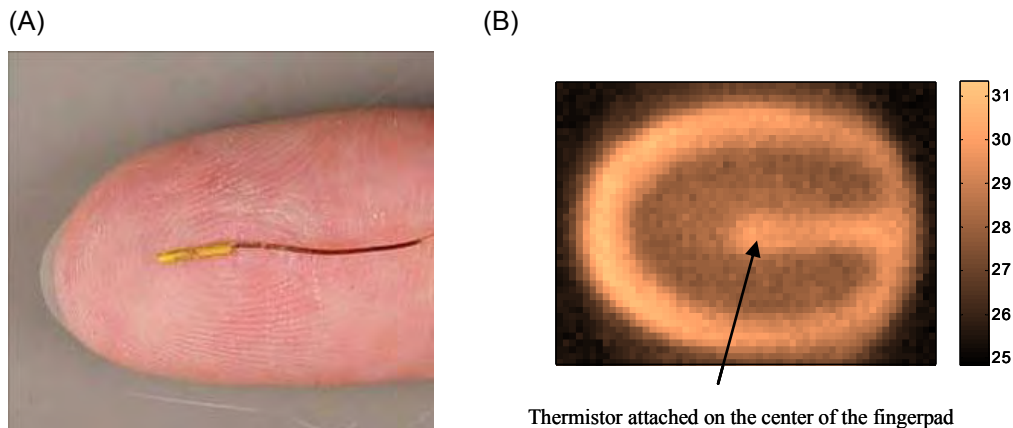


Figure 5. System evaluation with the insulation tape (A) and fingerpad (B) as the target.

After verifying that this thermal measurement system was able to provide accurate measurements, the thermal response of the fingerpad during contact with a thermistor attached to the center of the contact area was measured. The thermal image is shown in Figure 6. The outer grey section of the image is the background, and the white elliptical area is the fingerpad whose area is 225  $\text{mm}^2$ . The inner grey section inside the elliptical area indicates the region in which the skin temperature decreased during contact. The

white region indicated by the arrow shows how a small thermistor (457  $\mu\text{m}$  in diameter and 3.18 mm in length) can deform the fingerpad and influence the change in skin temperature during contact. The average temperature in the region of the thermistor was 29.6  $^{\circ}\text{C}$ , which is about 1.5  $^{\circ}\text{C}$  higher than the temperature in the rest of the contact area (28.1  $^{\circ}\text{C}$ ). The slight temperature gradient at the boundary of the inner grey section indicates that the decrease in skin temperature was localized within the contact area. This thermal image confirms the limitations of contact thermal sensors and suggests that the discrepancies noted between theoretical and measured changes in skin temperature may reflect measurement limitations and not the capabilities of the thermal model.



*Figure 6. An image of a fingerpad with a thermistor attached at the center of the contact area (A) and the corresponding thermal image when making contact with the contact material (B).*

## DISCUSSION

The two targets, insulation tape and the fingerpad used in the present study were both non-transparent and had emissivity values close to 1. Based on the relation  $\varepsilon + \tau + \rho = 1$ , the effect of the reflection of ambient radiation through the target surface was not significant, which greatly reduced the influence of the ambient condition on the measurement of the target temperature. The results of the emissivity check also indicated that using the overall average emissivity was appropriate for measuring the target temperature in the present thermal measurement system.

When the contact materials and beamsplitter were added to the system, the sources of radiation that could be detected by the infrared camera increased because those optics were able to transmit, reflect and emit thermal radiation. In order to simplify the problem, it was necessary to assume that the optics were gray bodies and to use their bandpass optical properties to derive the target temperature based on the IR model proposed in this study. Since the beamsplitter was inclined at an angle of 45 $^{\circ}$ , the effect of radiation bouncing back and forth between the contact material and beamsplitter was not significant and therefore was not considered in the IR model.

In order to validate the IR model and evaluate the thermal measurement system, calibration tests were conducted with the insulation tape and the fingerpad. During the test, the targets were placed as close to the contact material as possible without actually touching it. This made it possible to precisely monitor the temperature of the targets under conditions similar to the intended application. That is measuring the skin temperature when making contact.

As shown in Figure 6, the thermal sensors were not able to detect the full extent of the temperature change during contact even when they were attached to the center of the contact area. It is presumably this limitation that caused the measured change in skin temperature to be much lower than the model predictions (See Figure 1). In addition, the thermal sensor's own thermal mass may result in its insensitivity to the

instantaneous change in skin temperature upon contact, rendering it unable to capture the time course and amplitude of the change in skin temperature during contact as shown in Figure 1.

## SUMMARY

In this study, an infrared thermal measurement system was designed, fabricated and calibrated so that it could be used to assist in the development of a thermal display. The infrared thermal measurement system is able to provide a more accurate measurement of temperature without the limitations imposed by contact thermal sensors. The layout and optical arrangement of the system enables the measurement of the skin temperature distribution on the fingerpad together with contact force and contact area.

An IR model was proposed to account for the various sources of thermal radiation in order to derive the skin temperature based on the thermal energy detected by the infrared camera. Calibration tests with both insulation tape and the fingerpad as targets validated this IR model and confirmed that the thermal measurement system is able to provide accurate temperature measurements.

The infrared thermal measurement system required that the contact material be transparent in both the infrared and visible spectrum. It was therefore designed to assist in the development of the thermal model by providing a means for recording skin temperature more accurately during contact, and not as a system that would be integrated into a haptic interface. The thermal measurements recorded with the infrared thermal measurement system can then be compared directly to the model predictions of changes in skin temperature during contact to evaluate the validity of the model in predicting the changes in skin temperature during hand-object interactions.

## REFERENCES

- [1] S. Ino, S. Shimizu, T. Odagawa, M. Sato, M. Takahashi, T. Izumi, and T. Ifukube, "A tactile display for presenting quality of materials by changing the temperature of skin surface," presented at IEEE International Workshop on Robot and Human Communication, 1993.
- [2] A. Yamamoto, B. Cros, H. Hasgimoto, and T. Higuchi, "Control of thermal tactile display based on prediction of contact temperature," presented at Proceedings of the IEEE International Conference on Robotics and Automation, 2004.
- [3] H.-N. Ho and L. A. Jones, "Material identification using real and simulated thermal cues," presented at Proceedings of 26th Annual International Conference of the IEEE Engineering in Medicine and Biology Society, 2004.
- [4] H.-N. Ho and L. A. Jones, "Contribution of thermal cues to material discrimination and localization," *Perception & Psychophysics*, vol. 68, pp. 118-128, 2006.
- [5] H.-N. Ho and L. A. Jones, "Thermal model for hand-object interactions," presented at Proceedings of the IEEE Symposium on Haptic Interfaces for Virtual Environment and Teleoperator Systems, 2006.
- [6] F. P. Incropera and D. P. DeWitt, *Fundamentals of Heat and Mass Transfer*. New York: Wiley, 1996.
- [7] G. Gaussorgues, in *Infrared Thermography*. New York: Chapman & Hall, 1994.
- [8] R. P. Madding, "IR window transmittance temperature dependence," presented at Proceedings of InfraMation, 2004.
- [9] R. P. Madding, "Spectrally transmissive IR windows – how they affect your thermography results," presented at Proceedings of SPIE, 2005.

## ACKNOWLEDGEMENTS

Supported through ADA CTA by the U.S. Army Research Laboratory under Cooperative Agreement DAAD19-01-2-0009.